HOSTED BY

ELSEVIER

Available online at www.sciencedirect.com

ScienceDirect

journal homepage: http://ees.elsevier.com/ejbas/default.asp

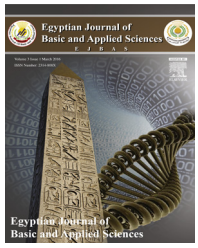

Full Length Article

Synthesis and characterization of Hg(II) and Cd(II) complexes derived from the novel acenaphthaquinone-4-phenyl thiosemicarbazone and its CPE application

Ibrahim M. Kenawy [a], *Mohamed M. Hassanien* [b], *Mohamed H. Abdel-Rhman* [a,*], *Rania R. Zaki* [a], *Hala S. Rashed* [a]

[a] *Chemistry Department, Faculty of Science, Mansoura University, Mansoura, Egypt*
[b] *Chemistry Department, Industrial Education College, Beni-Suef University, Beni-Suef, Egypt*

ARTICLE INFO

Article history:
Received 30 August 2015
Received in revised form 25 October 2015
Accepted 27 October 2015
Available online 16 November 2015

Keywords:
Acenaphthaquinone
Thiosemicarbazone
Separation and preconcentration
CPE

ABSTRACT

The new acenaphthaquinone-4-phenyl thiosemicarbazone (APTH) was synthesized. The reaction of Hg(II) and Cd(II) chloride with APTH yields bimetallic complexes, which are characterized by elemental, IR, UV-Vis., ^{1}H-NMR and Mass spectroscopy. The APTH employed as a chelating agent for CPE procedure of trace amounts of mercury and cadmium from aqueous medium. The Hg(II) and Cd(II) is preconcentrated using 0.1% w/v Triton X-114 and 2×10^{-5} M APTH at pH 7. The calibration curve is linear in the ranges 0.25–3 and 0.25–7.5 ng/ml for Cd(II) and Hg(II), respectively. The proposed method was applied successfully in the determination of Hg(II) and Cd(II) in different water samples.

1. Introduction

Thiosemicarbazones is an important class of NS donors due to their variable donor properties, structural diversity and biological applications [1]. They got biological importance from the fact that they have good antiparasital [2], antibacterial [3], antitumor [4,5], antimalarial [6], antineoplastic [7] and antivira1 [8] activities. Chelation of some thiosemicarbazones to some metal ions increase their antitumor activity [9,10]. Since, the chemical nature of thiosemicarbazone derivatives and their metal complexes have been widely investigated [11–15]. Thiosemicarbazones have been used for extraction and determination of some metal ions in biological and pharmacological samples [16,17].

Acenaphthaquinone used as an intermediate for the manufacturing of dyes, pharmaceuticals, pesticides, and synthesis of versatile fluorescent chemosensors when reacts with

* *Corresponding author.* Tel.: +201006192777.
E-mail address: mhassan2371@yahoo.com (M.H. Abdel-Rhman).
http://dx.doi.org/10.1016/j.ejbas.2015.10.001

Table 1 – Analytical and physical data of APTH and its complexes.

Compound	m.p. (°C)	Color	Elemental analyses; found (Calcd.)			Λ_m[a]
			C	H	M	
APTH	190	Brown	68.13 (68.86)	3.79 (3.95)	–	–
$[Cd_2(APTH)Cl_4]$	175	Red break	33.35 (32.69)	2.13 (1.88)	32.89 (32.21)	5.47
$[Hg_2(APTH)_2Cl_4(EtOH)_2]$	215	Reddish brown	39.11 (38.87)	2.51 (2.95)	31.18 (30.91)	18.50

[a] $Ohm^{-1}.cm^2.mol^{-1}$.

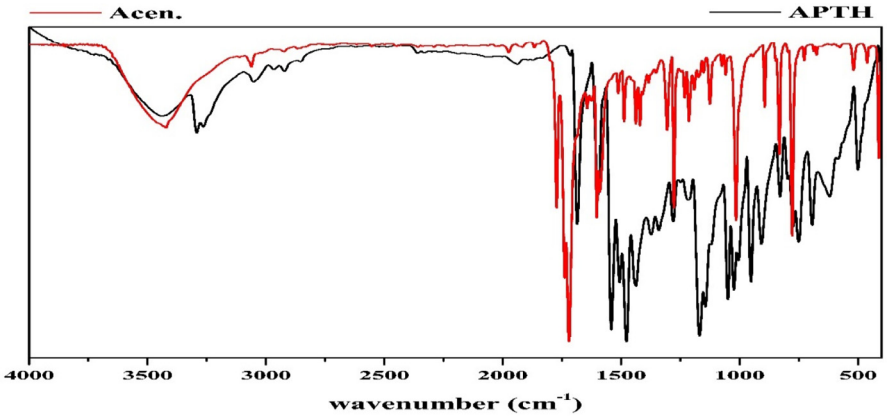

Fig. 1 – IR spectrum of APTH in comparison to acenaphthoquinone.

8-aminoquinoline [18]. Acenaphthaquinone thiosemicarbazone reacted with Fe(III), Ni(II), Cu(II) and Zn(II) chlorides or acetates leads to formation of complexes that have been characterized by spectroscopic studies. Also, the free ligand showed high activity of cell proliferation inhibition and induced differentiation on Friend erythroleukemia cells (FLC) [19].

Determination of trace metals in a complex matrix has been usually complicated. In such matrixes, separation and preconcentration steps should precede determination to minimize or even eliminate matrix effects and contaminants, lower the detection limit and enhance the detectability. Cloud point extraction (CPE), as an effective separation and preconcentration technique, was first studied by Watanabe and co-workers in the early 1980's [20–23]. The CPE have distinct merits of low cost, simplicity, speed, and lower toxicity to the environment than extractions using organic solvents, which have high capacity to concentrate wide variety of analytes, high recoveries, and high concentration factors. In the CPE technique, the surfactants used are mostly of nonionic type, such as Triton X-114, X-100, or PONPE. Triton X-114 is the most applied surfactant due to its low cloud-point temperature (30 °C), high density, commercial availability and lower toxicity [24].

Heavy metals like Cd(II) and Hg(II) are toxic [25,26] where the excess of Cd(II) leads to renal toxicity while Hg(II) leads to damage of the central nervous system and causes neuropsychiatric disorders [27]. Due to their low concentration in the environmental and biological samples, a preconcentration-separation technique is generally necessary prior to determination. For this purpose, various analytical procedures have been used such as adsorption on graphene oxide nanosheets [26], activated carbon [28,29], co-precipitation [30,31], *Streptococcus pyogenes* immobilized on Dowex Optipore SD-2 [32], column extraction [33,34], ion selective electrode [35,36], liquid–liquid extraction LLE [37], biosorbent *Staphylococcus aureus* [38], biomass *Drepanocladus revolvens* and *Xanthoparmelia conspersa* [39,40] and cloud-point extraction CPE [41,42].

In the present study, the new acenaphthaquinone-4-phenylthiosemicarbazone (APTH) and its complexes with Hg(II) and Cd(II) was synthesized and characterized. In addition, it is employed in CPE procedure for separation, preconcentration and determination of Cd(II) and Hg(II) in water samples.

Table 2 – Infrared spectral date of APTH and its metal complexes in KBr.

Assignment	APTH	$[Cd_2(APTH)Cl_4]$	$[Hg_2(APTH)_2Cl_4(EtOH)_2]$
$\nu(N^4H)$	3292	3290	3351
$\nu(N^2H)$	3263	3236	3293
$\nu(C=O)_{free}$	1690[a]	–	1702
$\nu(C=O)_{H\text{-}bonded}$	1680[a]	1675[a]	1683
$\nu(C=N^1)$	1660[a]	1655[a]	1620
$\nu(C=C)$	1600	1600	1600
Thioamide I	1540	1535	1577
Thioamide II	1430	1442	1456
Thioamide III	1168	1172	1174
$\nu(C=S)$	828	802	827
$\nu(N—N)$	1143	1145	1139
$\nu(C—O)$	1049	1025	1031
$\rho(NH)$	750	732	730,750

[a] Band obtained from deconvolution analysis.

Table 3 – Deconvolution analysis parameters of the APTH IR spectrum in the range 1710–1620 cm^{-1} (R^2 = 0.9986).

Peak type / No.	Center	Amplitude	FWHM	% Area
Gauss Amp 1	1660	4.94	39.41	32.81
Gauss Amp 2	1680	12.69	19.47	42.17
Gauss Amp 3	1690	9.97	14.71	25.02

2. Experimental

2.1. *Apparatus*

The IR spectra were recorded as KBr discs using Thermo-Nicolet IS10 FTIR Spectrometer (Thermo Fisher Scientific Inc, Waltham, MA, USA). The electronic spectra were measured on a Unicam UV-Vis Spectrometer UV2 (Akribis Scientific Ltd., Cheshire, WA16 0JG, United Kingdom). The ^{1}H-NMR spectra of APTH and its Cd(II) complex, in DMSO-d_6, were recorded on Jeol Delta2 Spectrometer (500 MHz) (JEOL USA Inc., Peabody, MA 01960, USA). The mass spectrum of APTH was measured by Thermo DSQ II Spectrometer (Thermo Fisher Scientific Inc., Waltham, MA, USA). The FAAS measurements were carried out using A Perkin Elmer Analyst 800 atomic absorption spectrometer (Perkin Elmer Inc., Waltham, MA 02451, USA) with a longitudinal Zeeman background correction furnished with a transversely heated graphite atomizer (THGA), which was used for the determination of Cd(II) at wavelength 228.8 nm, slit width 0.7 nm and lamp current 12 mA. Sample solutions were injected into the atomizer by using AS-800 auto-sampler. The sample injection volume was 20 µl. The system is equipped with winLab 32 software. The Hg(II) was determined by cold vapor technique (CVAAS) using 1% m/v $NaBH_4$ in 0.05% m/v NaOH at carrier gas flow rate of 1000 ml/min and slit width 0.7 nm. The pH of the solution was adjusted using Hanna instrument model 8519 digital pH meter (HANNA Instruments, Rhode Island, Woonsocket, RI 02895, USA). The temperature of the cell compartment was kept constant by circulating water from a thermostatic water bath at the desired temperature, which was used for the CPE experiments (Memmert GmbH Co. KG, D-91126 Schwabach, Germany). A centrifuge was used to accelerate the phase separation process employing Centrifuge Hematocrit Mikro set (Alkeslabindo, Kota Depok, Indonesia).

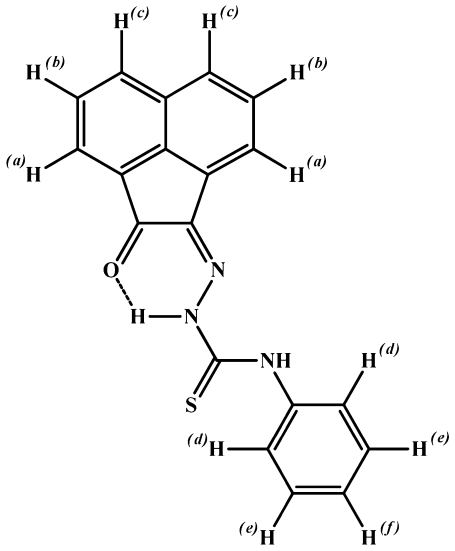

Structure 1 – Structure of APTH.

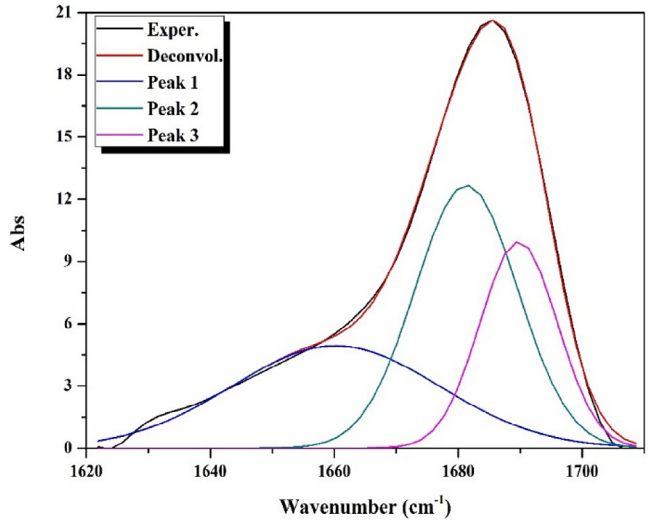

Fig. 2 – IR deconvolution analysis of APTH in the range 1710–1620 cm^{-1}.

2.2. *Reagents and solutions*

All chemicals purchased from Aldrich (Sigma-Aldrich Chemie GmbH, Munich, Germany) were of analytical grade quality and used without purification. Distilled water was used in all experiments. The stock solution of 10^{-4} M $CdCl_2$ and $HgCl_2$ was prepared by dissolving 0.0660 and 0.0027 g, respectively, in 100 ml distilled water in a measuring flask. The non-ionic surfactant, Triton X-114, was used without further purification. The stock solution 1% w/v was prepared by dissolving 1 g of Triton X-114 in 100 ml distilled water. Hexamine buffer solutions 0.5 M,

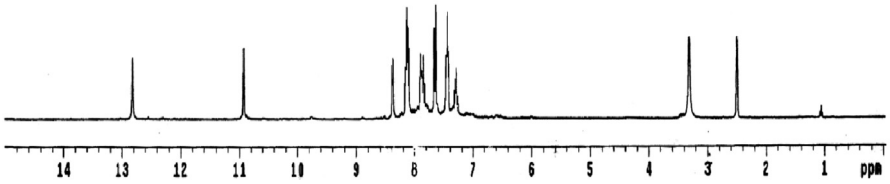

Fig. 3 – ^{1}H-NMR spectrum of APTH.

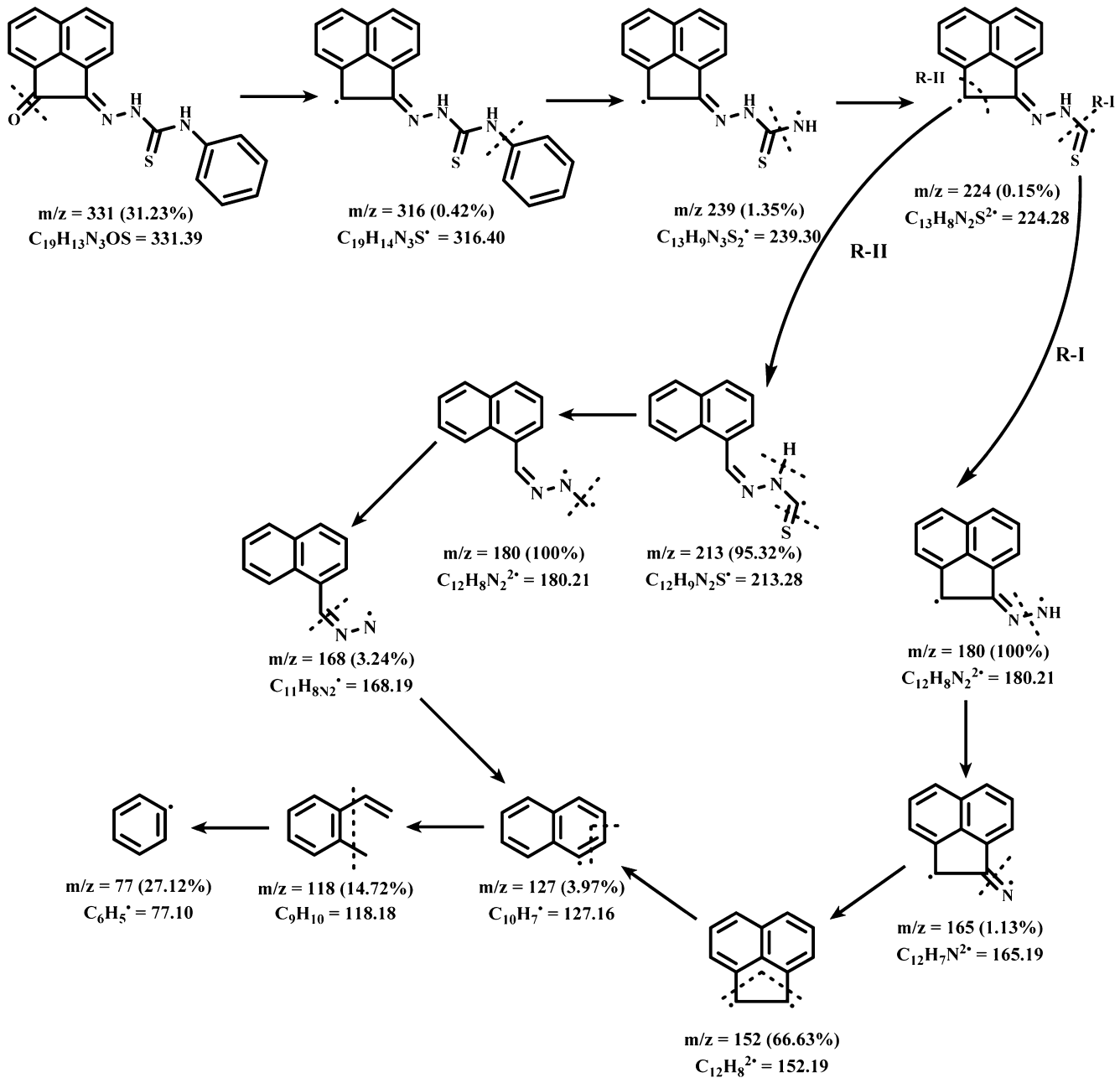

Scheme 1 – Fragmentation pattern of APTH.

pH 4-8, were prepared by dissolving 17.5240 g in 250 ml distilled water in a measuring flask. A 0.1 M NaOH and/or HNO_3 solution used to adjust the pH to the desired value. For pH 9 and 10, ammonium chloride/ammonium hydroxide buffer solution was used. A stock solution of the ligand (APTH) 10^{-3} M was prepared by dissolving 0.0331 g in 100 ml acetone.

2.3. *Preparation of the ligand and solid complexes*

The acenaphthaquinone-4-phenylthiosemicarbazone (APTH) was prepared by heating under reflux a mixture of acenaphthaquinone (0.01 mol, 1.82 g) and 4-phenylthiosemicarbazide (0.01 mol, 1.67 g) in ethanol in the presence of 5 ml glacial acetic acid for 1 h. On cooling, a fine brown powder was formed, filtered off, and washed successfully with EtOH and then diethyl ether, and recrystallized from EtOH (m.p. 190 °C; yield 91%).

The metal complexes prepared by reacting the APTH (0.001 mol, 0.331 g) with the equivalent amount of $CdCl_2.2.5H_2O$ and $HgCl_2$ salts were dissolved in EtOH under reflux for 2 h after. A red break and reddish brown precipitate were formed in case of Cd(II) and Hg(II), respectively, filtered off while hot, washed successfully with hot ethanol and then diethyl ether, and dried and preserved in a vacuum desiccator over anhydrous calcium chloride (for Cd(II); m.p. 275 °C, yield 96%; for Hg(II), m.p. 215 °C, yield 93%).

2.4. CPE procedure

For the CPE, an aliquot of 10 ml of a solution containing Cd(II) or Hg(II), Triton X-114 (0.1% w/v), 2×10^{-5} M APTH and 2 ml of buffer solution (pH = 7), were kept for 10 min in a thermostatic bath at 45 °C. Subsequently, separation of the phases was achieved by centrifugation for 10 min at 4000 rpm. The phases were cooled down in an ice bath in order to increase the viscosity of the surfactant rich phase. The bulk aqueous phase was easily decanted simply by inverting the tube. The surfactant-rich phase was made up to 0.5 ml by adding absolute methanol. The absorbance was measured at 478 and 446 nm for Cd(II) and Hg(II), respectively.

2.5. Sample preparation

First, the water samples from different origin were filtered through filter paper to separate the coarse particles and suspended matter, and second, through a Millipore cellulose nitrate membrane (pore size 0.45 μm), then acidified to pH 2 with HNO_3 and stored in a refrigerator in a dark polyethylene bottle.

3. Result and discussion

The reaction of the ligand with the chloride salt of Cd(II) and Hg(II) led to formation of bimetallic complexes which its elemental analyses indicate that have the formula $[Cd_2(APTH)Cl_4]$ (red break) and $[Hg_2(APTH)_2Cl_4(EtOH)_2]$ (reddish brown) respectively (Table 1).

3.1. Characterization of APTH

The comparison of the APTH infrared spectrum with that of the acenaphthylene-1,2-dione, as shown in Fig. 1, indicated that four new bands were observed at 3292, 3263, 1143 and 750 cm^{-1}, and attributed to $\nu(N^4H)$, $\nu(N^2H)$, $\nu(N—N)$ and $\rho(NH)$ [43] vibrations, respectively. Another four bands were observed at 1540, 1430, 1168 and 828 cm^{-1} and assigned to Thioamide I, II, III and $\nu(C=S)$ [44], respectively (Table 2). The broad band observed in 1710–1620 cm^{-1} region consisted of three overlapped bands according the deconvolution analysis data (Table 3). The first one at 1690 cm^{-1} was attributed to the $\nu(C=O)$ while the second at 1680 cm^{-1} was due to the $\nu(C=O)$ involved in hydrogen bond. The third one at 1660 cm^{-1} was assigned to $\nu(C=N^1)$ vibration (Fig. 2). The existence of a shoulder at 3238 cm^{-1} in addition to a weak band at 1937 cm^{-1} suggest the involvement of the $C=O$ and N^2H in intramolecular hydrogen bond [45] (Table 2).

The ^{1}H-NMR spectrum of the ligand in DMSO-d_6 shows two singlet signals at 12.82 and 10.93 ppm attributed to protons of N^4H and N^2H [19], respectively. Addition of D_2O to the solution of the ligand leads to disappearance of these two signals, confirming its assignment. Also, the spectrum displayed three triplet signals at 7.45, 7.87 and 8.12 ppm assigned to the protons at positions (*f*), (*b*) and (*e*) [44], respectively. Moreover, the spectrum shows three doublet signals at 7.32, 7.65 and 8.37 ppm attributed the protons at (*d*), (*a*) and (*c*) positions [44], respectively (Fig. 3) (Structure 1).

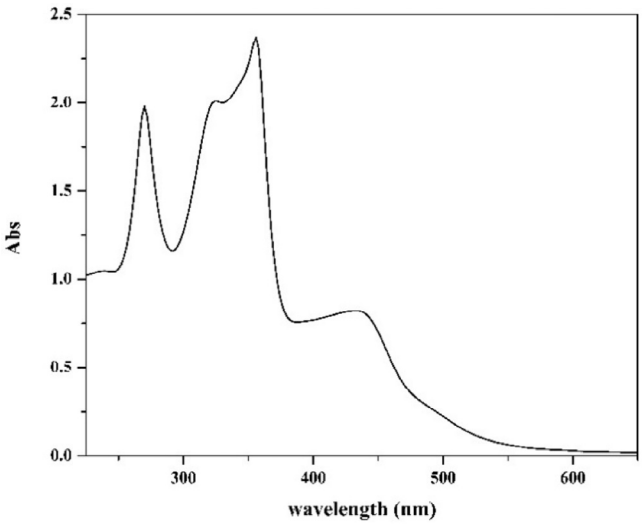

Fig. 4 – Electronic spectrum of APTH.

The mass spectrum of APTH showed a molecular ion peak at (m/z = 331; 31.23%), which coincides with its molecular weight (331.39). The suggested fragmentation pattern, shown in Scheme 1, indicated that there were two routes by which fragmentation may occur, showing base peak at m/z = 180 corresponding to the formula $C_{12}H_8N_2$ (180.21).

Finally, the electronic spectrum of the ligand in DMSO showed four bands at 37,040, 30,675, 28,090 and 23,255 cm^{-1} with a shoulder at 19,840 cm^{-1}. The first two bands were attributed to $\pi \rightarrow \pi^*$ transitions of the aromatic rings, $C=O$, $C=N^1$ and $C=S$ [43] while the other three bands were attributed to $n \rightarrow \pi^*$ transitions of carbonyl, azomethine and $C=S$ groups [45,46], respectively (Fig. 4).

3.2. Characterization of metal complexes

The spectrum of $[Cd_2(APTH)Cl_4]$ complex, in KBr disc, displayed band at 3236 cm^{-1} with a shoulder at 3292 cm^{-1} in

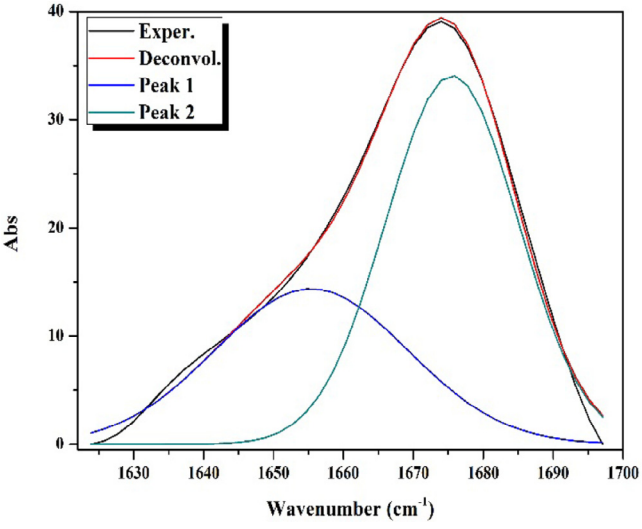

Fig. 5 – IR deconvolution analysis of $[Cd_2(APTH)Cl_4]$ in the range 1700–1620 cm^{-1}.

Table 4 – Deconvolution analysis parameters of the $[Cd_2(APTH)Cl_4]$ IR spectrum in the range 1700–1620 cm^{-1} (R^2 = 0.9966).

Peak type / No.	Center	Amplitude	FWHM	% Area
Gauss Amp 1	1655	14.37	32.42	38.08
Gauss Amp 2	1675	34.08	22.23	61.92

addition to two bands at 1145 and 732 attributed to $\nu(N^2H)$, $\nu(N^4H)$ [46], $\nu(N—N)$, and $\rho(NH)$ [43] vibrations, respectively. Moreover, four bands were observed at 1535, 1442, 1172 and 802 cm^{-1} assigned Thioamide I, II, III and $\nu(C=S)$ [44], respectively. The deconvolution analysis of the broad band centered at 1673 cm^{-1}, shown in Fig. 5, indicated that it consisted of two overlapped bands at 1675 and 1655 cm^{-1} attributed to $\nu(C=O)$ [47] and $\nu(C=N^1)$ [48] vibrations, respectively (Table 4). The comparison of the spectral data with that belonging to the ligand clears that $\nu(N^2H)$, $\nu(C=O)$, $\nu(C=N^1)$ and $\nu(C=S)$ are shifted to lower wavenumbers suggesting its involvement in coordination to the metal ion [49] (Table 2). Therefore, it could be concluded that the ligand is coordinated to the metal ion in neutral tetradentate manner and exists in keto-form (Structure 2).

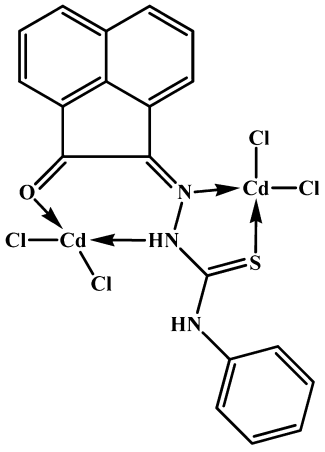

Structure 2 – Structure of Cd(II) complex.

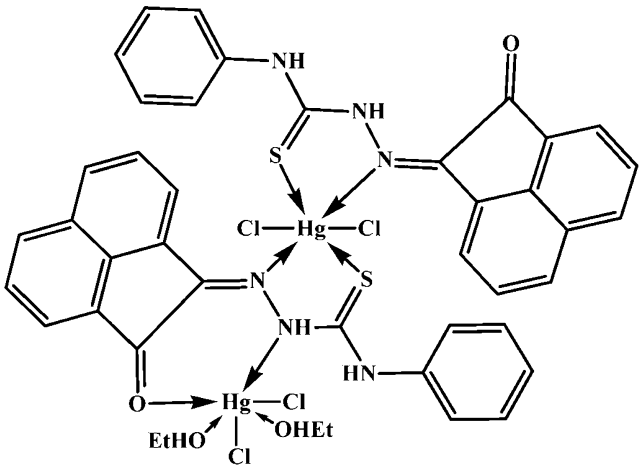

Structure 3 – Structure of Hg(II) complex.

On the other hand, the $[Hg_2(APTH)_2Cl_4(EtOH)_2]$ spectrum showed a broad band centered at 3450 cm^{-1} attributed to the $\nu(OH)$ of the ethanol molecules. The appearance of the $\nu(N^4H)$ band at 3290 cm^{-1} indicates that it did not participate in coordination to the metal ion [46] (Fig. 6). A band at 3351 cm^{-1} and shoulder at 3264 cm^{-1} were attributed to $\nu(N^2H)$ [49] involved in coordination to the metal ion and the free one, respectively. Moreover, two bands at 1706 and 1683 cm^{-1} were observed and attributed to $\nu(C=O)$ coordinated to metal ion [47] and $\nu(C=O)$ free, respectively. The $\nu(C=N^1)$ vibration band observed at 1620 [49] cm^{-1} indicating its participation in coordination to metal ion. All these spectral data clears out that the ligand exists in keto-form [46]. Thus, the appearance of two bands due to $\nu(N^2H)$ and $\nu(C=O)$ vibrations corresponding to the free and coordinated groups was taken as evidence for that one ligand molecule coordinated to the metal ion as neutral tetradentate while the other is neutral bidentate (Structure 3) (Table 2).

Moreover, the ^{1}H-NMR spectrum of Cd(II) complex in DMSO-d_6, in comparison to that of the ligand, shows the aromatic protons at more or less the same positions in addition to singlet signals at 12.83 and 10.84 ppm attributed to the N^2H and N^4H protons, respectively. The appearance of the N^4H at the same

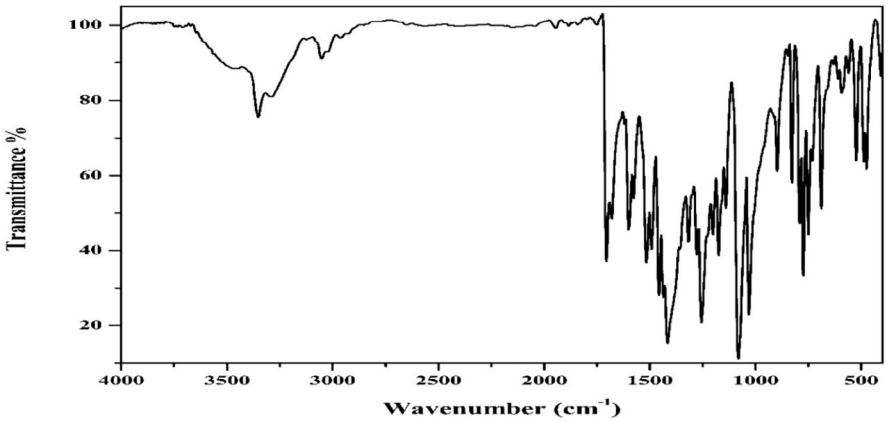

Fig. 6 – IR spectrum of $[Hg_2(APTH)_2Cl_4(EtOH)_2]$.

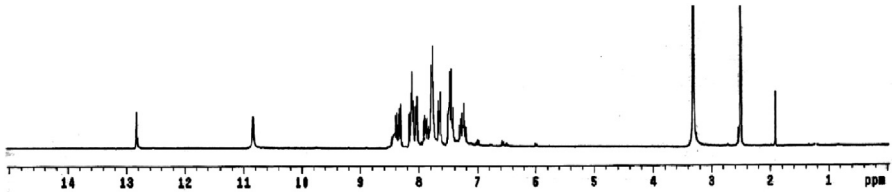

Fig. 7 – ^{1}H-NMR spectrum [Cd_2(APTH)Cl_4] complex.

position and the shift of N^2H to upfield (~0.1 ppm) confirm the involvement of N^2H in coordination to the metal ion (Fig. 7).

The electronic spectrum of Cd(II) complex in DMSO showed three bands at 36,230, 32,050 and 27,930 cm^{-1} attributed $\pi\rightarrow\pi^*$ of the aromatic rings, $\pi\rightarrow\pi^*$ of C = O and $n\rightarrow\pi^*$ of C = O [43,45,46], respectively. Also, a band at 20,000 cm^{-1} was observed with two shoulders at 23,255 and 21,460 cm^{-1} and assigned to ligand to metal charge transfer [50] and $n\rightarrow\pi^*$ of azomethine groups, respectively. The shift in band position of the carbonyl transition confirms the involvement of carbonyl group in coordination to the metal ion. Finally, the spectrum of Hg(II) complex displayed three bands at 33,780, 27,780 and 19,840 cm^{-1} with three shoulders at 31,850 and 23,925 cm^{-1} due to intra-ligand transitions. Moreover, a new band at 21,000 cm^{-1} was observed and attributed to LMCT transition. The data confirm the existence of the ligand in keto form.

3.3. *Cloud point extraction*

3.3.1. *Effect of pH on CPE*

The extraction of metal ions using cloud point technique involves formation of a complex with the reagent used that has sufficient hydrophobic nature to be extracted into a small volume of surfactant-rich phase and so obtaining the desired preconcentration. The pH plays a unique role in metal-chelate formation and subsequent extraction [51]. Fig. 8 shows the influence of pH on the absorbance of the Cd(II) and Hg(II) complexes at 478 and 446 nm, respectively. As seen, both metals can be extracted efficiently at pH 7 after which the complexation and/or extraction of the metal ion decreased. The Hg(II) shows higher stability than Cd(II), which has a sharp decrease. Hence, pH 7 was chosen as the working pH.

3.3.2. *Effect of APTH concentration*

The effect of concentration of APTH on analytical response is shown in Fig. 9. As seen, the absorbance increases, reaching maximum at 2×10^{-5} M, which is considered as complete chelation and extraction of both metals Cd(II) and Hg(II). From the data, the optimum concentration used for further studies is 2×10^{-5} M.

3.3.3. *Effect of Triton X-114 concentration*

The plot of the recovery percentage versus the concentration of Triton X-114 is shown in Fig. 10. At a concentration of 0.1% (w/v), optimum recovery of the analytes is obtained. At lower concentrations, the extraction of chelated metal ions is low probably because of the inadequacy of the surfactant micelles to entrap the hydrophobic complex formed quantitatively. Increasingly, after this optimal concentration, the recovery is observed to decrease, which may be attributed to the increase in the final volume of the surfactant that causes the preconcentration factor (phase volume ratio) to decrease [52].

3.3.4. *Effect of the equilibration temperature and centrifugation time*

Optimal incubation time and equilibration temperature are necessary to complete reactions and to achieve easy phase

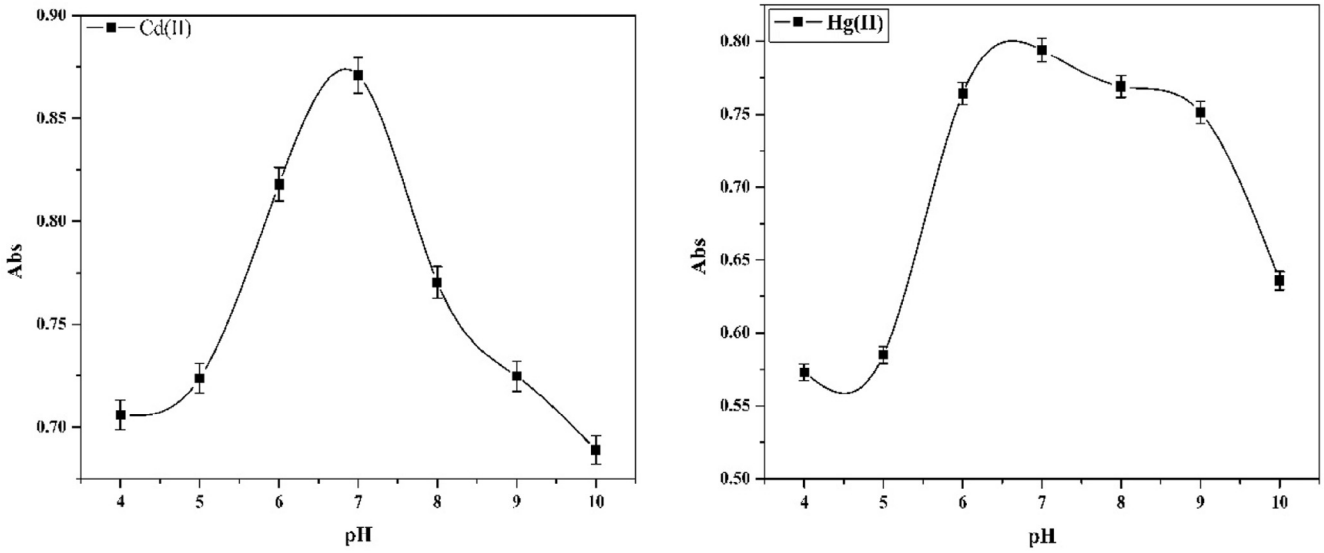

Fig. 8 – Effect of pH on the extraction recovery of Cd(II) and Hg(II) using APTH (10^{-5} M) and Triton X-114 (0.1 % w/v).

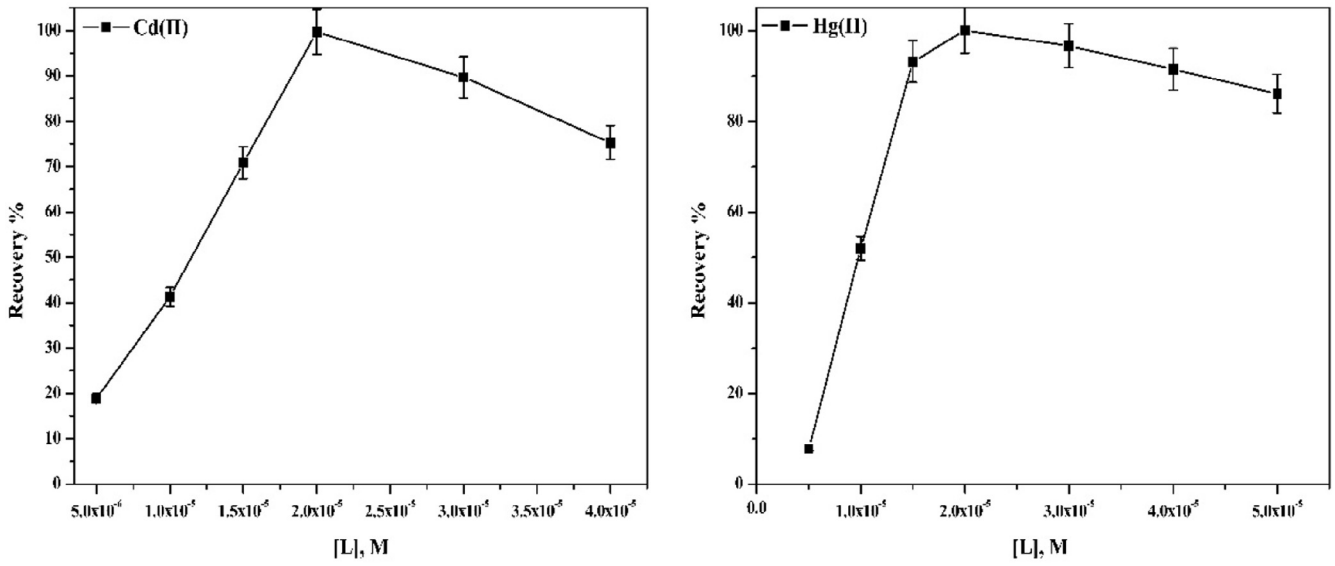

Fig. 9 – Effect of APTH concentration on the extraction recovery of Cd(II) and Hg(II) using Triton X-114 (0.1 % w/v) at pH 7.

separation and preconcentration as efficient as possible. The greatest analyte preconcentration factors are expected under conditions where the CPE is conducted using temperatures that are well above the cloud point temperature of the surfactant. It was found that a temperature of 45 °C is adequate for the analytes (Fig. 11).

It was desirable to employ the shortest equilibration time and the lowest possible equilibration temperature, which compromise the completion of reaction and efficient separation of phases. The dependence of absorbance upon equilibration and centrifugation times was studied within the range 5–25 min. The optimal time for equilibration and centrifugation is 10 min (Fig. 12).

3.3.5. *Figures of merit*

Under the optimum conditions, the increase of the metal concentration was studied in the range 0.25–10 ng/ml for Cd(II) and 0.25–25 ng/ml for Hg(II). The data indicated that the linear ranges are 0.25–3 and 0.25–7.5 ng/ml for Cd(II) and Hg(II), respectively; LOD = 1.0 and 2.0 ng/ml for Cd(II) and Hg(II), respectively; LOQ = 3.38 and 6.65 ng/ml for Cd(II) and Hg(II), respectively; % R.S.D. in the range 1.20–1.62 and phase volume ratio = 50 (Figs. 13 and 14). The detection limits (LODs) and limits of quantification (LQDs) calculation were based on the 3σ and 10σ criterion, respectively, where σ is the standard deviation of 5 determinations of the method carried out during the same analytical run. The blank was a 1% v/v ultrapure HNO_3 solution.

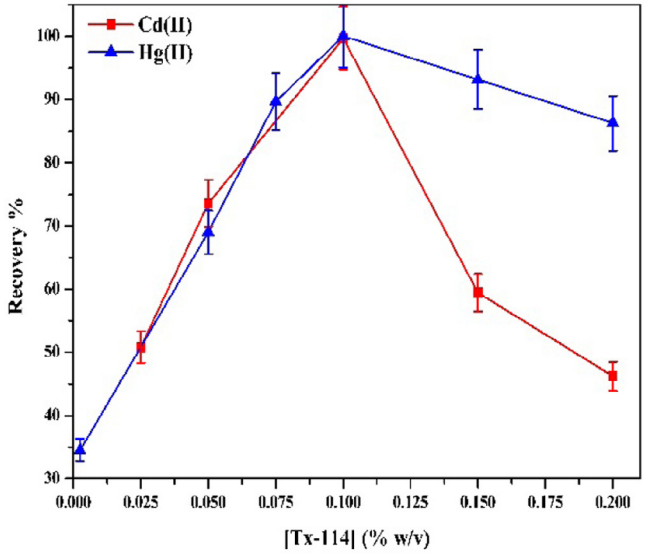

Fig. 10 – Effect of Triton X-114 concentration on the extraction recovery % of the Cd(II) and Hg(II) using APTH (2×10^{-5} M) at pH 7.

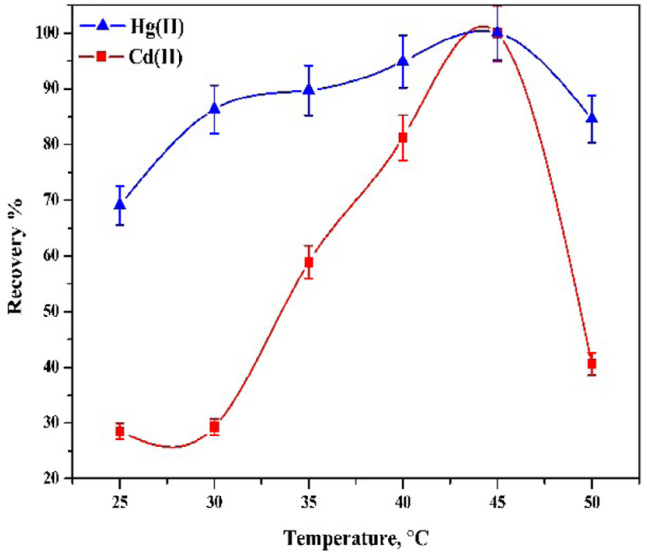

Fig. 11 – Effect of temperature on the extraction recovery % of the Cd(II) and Hg(II) using APTH (2×10^{-5} M) and Triton X-114 (0.1 %w/v) at pH 7.

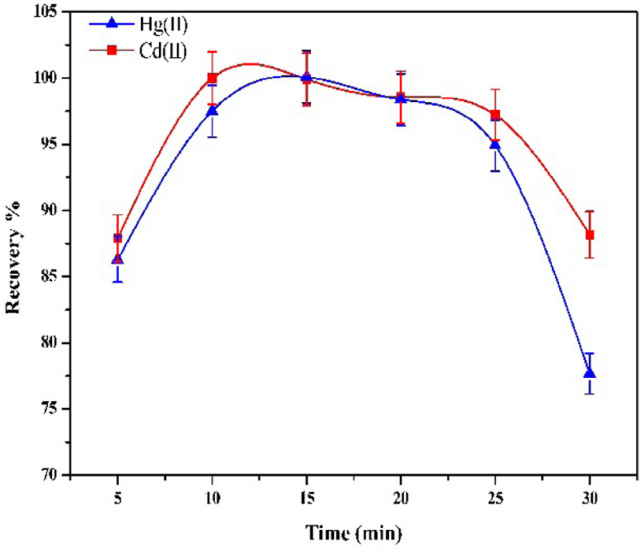

Fig. 12 – Effect of incubation time on the extraction recovery % of the Cd(II) and Hg(II) using APTH (2×10^{-5} M) and Triton X-114 (0.1 %w/v) at pH 7.

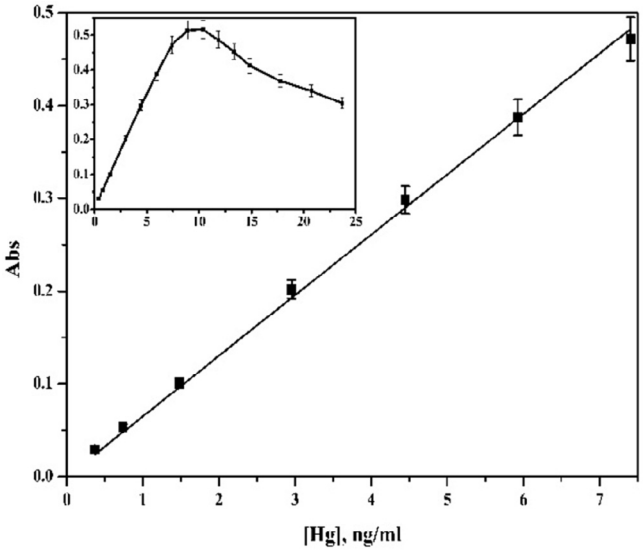

Fig. 14 – Calibration curve of the Hg(II) using APTH (2×10^{-5} M) and Triton X-114 (0.1 % w/v) at pH 7.

Repeatability (precision) was calculated as the relative standard deviation of five measurements of a sample with concentration values in the central region of the analytical range carried out during the same analytical run.

3.3.6. *Effect of interfering ions*

Two types of interference affect the preconcentration and/or the detection [53]. The effect of interfering ions at different concentrations on the absorbance of a solution containing 0.25 ppm of both Cd(II) and Hg(II) was studied. An ion was considered to interfere when its presence produced a variation in the absorbance of the sample of more than 5%. This increment of absorbance was evaluated for Cd(II) and Hg(II) at 478 and 446 nm, respectively, to establish the different effects of the interfering ions on the analytes. Among the tested interfering ions, Na^+, K^+, Cl^- and NO_3^- did not interfere at concentrations higher than that of the analytes by even more than 1000 fold while ions like Mg^{2+}, Ca^{2+}, I^-, PO_4^{3-} and SCN^- in addition to thiourea did not interfere at medium concentrations in the range 500–100 fold. On the other hand, Fe^{2+}, Fe^{3+},Al^{3+}, SO_4^{2-}, F^-, acetate and citrate show strong inference in concentration range 1–50 fold (Table 5).

3.3.7. *Analysis of real water samples*

The proposed CPE procedure was applied in determination of Cd(II) and Hg(II) from real water samples. The water samples were collected from tap water in Mansoura City, River Nile at

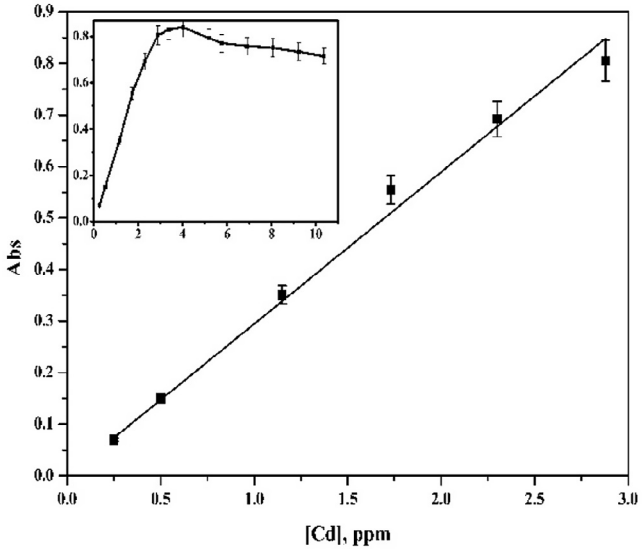

Fig. 13 – Calibration curve of the Cd(II) using APTH (2×10^{-5} M) and Triton X-114 (0.1 %w/v) at pH 7.

Table 5 – Tolerance limits for interference ions.

Interfering ion	Cd(II)		Hg(II)	
	Tolerance limit	Recovery %	Tolerance limit	Recovery %
K^+	1000	105.23	1000	99.46
Na^+	1000	101.87	1000	98.34
Mg^{2+}	1000	98.58	1000	100.34
Ca^{2+}	1000	99.92	1000	99.88
Fe^{2+}	1	98.63	1	99.69
Fe^{3+}	1	100.01	1	102.42
Al^{3+}	10	109.23	2	99.94
F^-	25	98.95	10	97.07
Cl^-	1000	98.23	1000	97.34
I^-	300	97.28	100	98.47
NO_3^-	1000	102.77	1000	99.93
SO_4^{2-}	100	103.22	100	99.69
PO_4^{3-}	80	99.67	30	98.22
SCN^-	150	99.50	50	97.64
Thiourea	200	96.50	100	97.79
Oxalate	20	98.18	1	98.55
Citrate	5	99.71	2	102.45

Table 6 – Determination of the Hg(II) and Cd(II) in 50 ml water samples using the presented CPE procedure in comparison with those obtained by FAAS.

Water sample (location)	Cd(II) (ng/ml)		Hg(II) (ng/ml)	
	Spectrophotometrically	FAAS	Spectrophotometrically	CVAAS
Tape (Mansoura)	0.15	0.145	0.12	0.11
River Nile (Mansoura)	0.03	0.03	0.05	0.04
El-Manzala lake (El-Manzala)	0.17	0.18	0.70	0.65
Mediterranean Sea (Gamasa)	0.22	0.21	0.34	0.35
Underground (Belqas territory)	0.13	0.14	0.17	0.16

Table 7 – CPE applications for metal ions analysis of the current work in comparison with previous studies.

Ion	Reagent	Surfactant	Detection system	DL (mg/l)	Matrix	References
Hg(II)	5-Br-PADAP	PONPE7.5	ETAAS	0.01	Human hair; urine and water	[54]
	APDC	TritonX-114	ICP-Ms	0.005	River, bottled, reservoir and tap water	[55]
	Dithiazone	TritonX-100	Spectrophotometry	0.014	Natural water	[56]
	PAN	TritonX-114	Spectrophotometry	1.65	River, lake and tap water	[57]
	APTH	TritonX-114	Spectrophotometry	2.0	River, lake, underground and tap water	Current work
Cd(II)	5-Br-PADAP	PONPE7.5	ETAAS	0.008	Urine, water	[58]
	APDC	TritonX-114	ICP-Ms	0.002	River, bottled, reservoir and tap water	[55]
	Dithiazone	TritonX-114	ICP-OES	0.093	Petroleum produced water	[57]
	PAN	TritonX-114	ICP-OES	4.0	Dolomite and bone ash	[58]
	APTH	TritonX-114	Spectrophotometry	1.0	River, lake, underground and tap water	Current work

Mansoura City, El-Manzala Lake, Mediterranean Sea at Gamasa, and underground water at Belqas territory. Hence, the determinations were carried out in spiked water samples with 1 ml of 20 ng/ml to 50 ml, assuming that the original content of this ions was negligible compared to the concentration spiked. The Hg(II) and Cd(II) content were determined spectrometrically and compared with those determined by HG-FAAS and FAAS, respectively. Table 6 shows the results of applying the proposed method on different water samples to determine the Cd(II) and Hg(II) contents. Finally, a comparison of the current work with previous studies is shown in Table 7. In case of Hg(II), the proposed procedure showed detection limit higher than the spectrophotometric determination using PAN as chelating agent (difference is 0.35 mg/l) [57]. In case of Cd(II), the detection limit of the proposed procedure is very close to ICP-OES determination using Dithiazone as chelating agent [57].

4. Conclusion

In this study the new acenaphthaquinone-4-phenyl thiosemicarbazone (APTH) and its bimetallic Hg(II) and Cd(II) complexes were synthesized and characterized. The chelation mode of the ligand to the metal ions is tetradentate as N,N,S,O donor. Applying the APTH as a chelating agent in CPE procedure for extraction of Hg(II) and Cd(II) from aqueous medium was achieved at pH 7 using 0.1% w/v Triton X-114 and 2×10^{-5} M APTH. Linear calibration curve is obtained in the ranges 0.25–3 and 0.25–7.5 ng/ml for Cd(II) and Hg(II), respectively. The method was applied successfully for determination of Hg(II) and Cd(II) in different water samples.

REFERENCES

[1] Gingras B, Somorjai R, Bayley C. The preparation of some thiosemicarbazones and their copper complexes. Can J Chem 1961;39(5):973–85.

[2] Du X, Guo C, Hansell E, Doyle PS, Caffrey CR, Holler TP, et al. Synthesis and structure-activity relationship study of potent trypanocidal thio semicarbazone inhibitors of the trypanosomal cysteine protease cruzain. J Med Chem 2002;45(13):2695–707.

[3] Kovala-Demertzi D, Demertzis MA, Filiou E, Pantazaki AA, Yadav PN, Miller JR, et al. Platinum (II) and palladium (II) complexes with 2-acetyl pyridine 4N-ethyl thiosemicarbazone able to overcome the cis-platin resistance. Structure, antibacterial activity and DNA strand breakage. Biometals 2003;16(3):411–18.

[4] Kovala-Demertzi D, Domopoulou A, Demertzis MA, Papageorgiou A, West DX. Palladium (II) complexes of 2-acetylpyridine N (4)-propyl, N (4)-dipropyl-and 3-hexamethyleneiminylthiosemicarbazones with potentially interesting biological activity. Synthesis, spectral properties, antifungal and in vitro antitumor activity. Polyhedron 1997;16(20):3625–33.

[5] Klayman D, Scovill J, Mason C, Bartosevich J, Bruce J, Lin AJ. 2-Acetylpyridine thiosemicarbazones. 6.2-Acetylpyridine and 2-butyrylpyridine thiosemicarbazones as antileukemic agents. Arzneimittelforschung 1982;33(7):909–12.

[6] Klayman DL, Scovill JP, Bartosevich JF, Mason CJ. 2-Acetylpyridine thiosemicarbazones. 2. N4, N4-Disubstituted derivatives as potential antimalarial agents. J Med Chem 1979;22(11):1367–73.

[7] Klayman DL, Scovill JP, Bartosevich JF, Bruce J. 2-Acetylpyridine thiosemicarbazones. 5. 1-[1-(2-Pyridyl) ethyl]-3-thiosemicarbazides as potential antimalarial agents. J Med Chem 1983;26(1):35–9.

[8] Shipman C, Smith SH, Drach JC, Klayman DL. Thiosemicarbazones of 2-acetylpyridine, 2-acetylquinoline, 1-acetylisoquinoline, and related compounds as inhibitors of herpes simplex virus in vitro and in a cutaneous herpes guinea pig model. Antiviral Res 1986;6(4):197–222.
[9] Turk SR, Shipman C, Drach JC. Selective inhibition of herpes simplex virus ribonucleoside diphosphate reductase by derivatives of 2-acetylpyridine thiosemicarbazone. Biochem Pharmacol 1986;35(9):1539–45.
[10] French FA, Blanz EJ. The carcinostatic activity of α-(N) heterocyclic carboxaldehyde thiosemicarbazones I. Isoquinoline-1-carboxaldehyde thiosemicarbazone. Cancer Res 1965;25(9 Pt 1):1454–8.
[11] Campbell MJ. Transition metal complexes of thiosemicarbazide and thiosemicarbazones. Coord Chem Rev 1975;15(2):279–319.
[12] Padhye S, Kauffman GB. Transition metal complexes of semicarbazones and thiosemicarbazones. Coord Chem Rev 1985;63:127–60.
[13] West DX, Liberta AE, Padhye SB, Chikate RC, Sonawane PB, Kumbhar AS, et al. Thiosemicarbazone complexes of copper (II): structural and biological studies. Coord Chem Rev 1993;123(1):49–71.
[14] Farrell N. Biomedical uses and applications of inorganic chemistry. An overview. Coord Chem Rev 2002;232(1):1–4.
[15] Lobana TS, Sharma R, Bawa G, Khanna S. Bonding and structure trends of thiosemicarbazone derivatives of metals – an overview. Coord Chem Rev 2009;253(7–8):977–1055.
[16] Ahmed SA. Alumina physically loaded by thiosemicarbazide for selective preconcentration of mercury (II) ion from natural water samples. J Hazard Mater 2008;156(1):521–9.
[17] Mahmoud ME, Yakout AA, Ahmed SB, Osman MM. Speciation, selective extraction and preconcentration of chromium ions via alumina-functionalized-isatin-thiosemicarbazone. J Hazard Mater 2008;158(2):541–8.
[18] Lodeiro C, Capelo JL, Mejuto JC, Oliveira E, Santos HM, Pedras B, et al. Light and colour as analytical detection tools: a journey into the periodic table using polyamines to bio-inspired systems as chemosensors. Chem Soc Rev 2010;39(8):2948–76.
[19] Rodriguez-Argüelles MC, Ferrari MB, Fava GG, Pelizzi C, Pelosi G, Albertini R, et al. Acenaphthenequinone thiosemicarbazone and its transition metal complexes: synthesis, structure, and biological activity. J Inorg Biochem 1997;66(1):7–17.
[20] Watanabe H, Tanaka H. A non-ionic surfactant as a new solvent for liquid – liquid extraction of zinc (II) with 1-(2-pyridylazo)-2-naphthol. Talanta 1978;25(10):585–9.
[21] Welleman J, Hulsbergen F, Verbiest J, Reedijk J. Influence of alkyl chain length in N-alkyl imidazoles upon the complex formation with transition-metal salts. J Inorg Nucl Chem 1978;40(1):143–7.
[22] Saitoh T, Kimura Y, Kamjdate T, Watanabe H, Haraguchi K. Distribution equilibria of metal chelates with thiazolylazo dyes between two phases formed from an aqueous micellar solution of a nonionic surfactant. Analytical Sciences 1989;5(5):577–81.
[23] Watanabe H, Saitoh T, Kamidate T, Haraguchi K. Distribution of metal chelates between aqueous and surfactant phases separated from a micellar solution of a nonionic surfactant. Microchim Acta 1992;106(1–2):83–90.
[24] Pytlakowska K, Kozik V, Dabioch M. Complex-forming organic ligands in cloud-point extraction of metal ions: a review. Talanta 2013;110:202–28.
[25] Duruibe J, Ogwuegbu M, Egwurugwu J. Heavy metal pollution and human biotoxic effects. Int J Phys Sci 2007;2(5):112–18.
[26] Zhao G, Li J, Ren X, Chen C, Wang X. Few-layered graphene oxide nanosheets as superior sorbents for heavy metal ion pollution management. Environ Sci Technol 2011;45(24):10454–62.
[27] Roat-Malone RM. Bioinorganic chemistry: a short course. Hoboken, New Jersey: John Wiley & Sons; 2007.
[28] Jankowski K, Yao J, Kasiura K, Jackowska A, Sieradzka A. Multielement determination of heavy metals in water samples by continuous powder introduction microwave-induced plasma atomic emission spectrometry after preconcentration on activated carbon. Spectrochim Acta Part B At Spectrosc 2005;60(3):369–75.
[29] Cerutti S, Moyano S, Marrero J, Smichowski P, Martinez L. On-line preconcentration of nickel on activated carbon prior to its determination by vapor generation associated to inductively coupled plasma optical emission spectrometry. J Anal At Spectrom 2005;20(6):559–61.
[30] Umashankar V, Radhamani R, Ramadoss K, Murty D. Simultaneous separation and preconcentration of trace elements in water samples by coprecipitation on manganese dioxide using D-glucose as reductant for KMnO(4). Talanta 2002;57(6):1029–38.
[31] Doner G, Ege A. Determination of copper, cadmium and lead in seawater and mineral water by flame atomic absorption spectrometry after coprecipitation with aluminum hydroxide. Anal Chim Acta 2005;547(1):14–17.
[32] Tuzen M, Uluozlu OD, Karaman I, Soylak M. Mercury (II) and methyl mercury speciation on *Streptococcus pyogenes* loaded Dowex Optipore SD-2. J Hazard Mater 2009;169(1):345–50.
[33] Tewari P, Singh AK. Preconcentration of lead with Amberlite XAD-2 and Amberlite XAD-7 based chelating resins for its determination by flame atomic absorption spectrometry. Talanta 2002;56(4):735–44.
[34] Jain VK, Mandalia HC, Gupte HS, Vyas DJ. Azocalix [4] pyrrole Amberlite XAD-2: New polymeric chelating resins for the extraction, preconcentration and sequential separation of Cu (II), Zn (II) and Cd (II) in natural water samples. Talanta 2009;79(5):1331–40.
[35] Gholivand MB, Mohammadi M. Khodadadian M, Rofouei MK. Novel platinum (II) selective membrane electrode based on 1, 3-bis (2-cyanobenzene) triazene. Talanta 2009;78(3):922–8.
[36] Li X-G, Ma X-L, Huang M-R. Lead (II) ion-selective electrode based on polyaminoanthraquinone particles with intrinsic conductivity. Talanta 2009;78(2):498–505.
[37] Camino M, Bagur M, Sanchez-Vinas M, Gazquez D, Romero R. Multivariate optimization of solvent extraction of Cd (II), Co (II), Cr (VI), Cu (II), Ni (II), Pb (II) and Zn (II) as dibenzyldithiocarbamates and detection by AAS. J Anal At Spectrom 2001;16(6):638–42.
[38] Tuzen M, Karaman I, Citak D, Soylak M. Mercury (II) and methyl mercury determinations in water and fish samples by using solid phase extraction and cold vapour atomic absorption spectrometry combination. Food Chem Toxicol 2009;47(7):1648–52.
[39] Sari A, Tuzen M. Removal of mercury (II) from aqueous solution using moss (*Drepanocladus revolvens*) biomass: equilibrium, thermodynamic and kinetic studies. J Hazard Mater 2009;171(1):500–7.
[40] Tuzen M, Sari A, Mendil D, Soylak M. Biosorptive removal of mercury (II) from aqueous solution using lichen (*Xanthoparmelia conspersa*) biomass: kinetic and equilibrium studies. J Hazard Mater 2009;169(1):263–70.
[41] Zhao L, Zhong S, Fang K, Qian Z, Chen J. Determination of cadmium (II), cobalt (II), nickel (II), lead (II), zinc (II), and copper (II) in water samples using dual-cloud point extraction and inductively coupled plasma emission spectrometry. J Hazard Mater 2012;239:206–12.
[42] Xu H, Zhang W, Zhang X, Wang J, Wang J. Simultaneous preconcentration of cobalt, nickel and copper in water samples by cloud point extraction method and their

determination by flame atomic absorption spectrometry. Proc Environ Sci 2013;18:258–63.
[43] Hassanien M, Gabr I, Abdel-Rhman M, El-Asmy A. Synthesis and structural investigation of mono-and polynuclear copper complexes of 4-ethyl-1-(pyridin-2-yl) thiosemicarbazide. Spectrochim Acta A Mol Biomol Spectrosc 2008;71(1):73–9.
[44] Silverstein R, Webster F. Spectrometric identification of organic compounds. Hoboken, New Jersey: John Wiley & Sons; 2006.
[45] Abdel-Rhman MH, Hassanian MM, El-Asmy AA. Spectral and structural density functional theory on 4-ethyl and 4-(p-tolyl)-1-(pyridin-2-yl)thiosemicarbazides and their Pd(II) complexes. J Mol Struct 2012;1019:110–19.
[46] El-Asmy AA, Hassanian MM, Abdel-Rhman MH. Synthesis, characterization and antibacterial activity of Pd (II), Pt (II) and Ag (I) complexes of 4-ethyl and 4-(p-tolyl)-1-(pyridin-2-yl) thiosemicarbazides. J Sulfur Chem 2010;31(2):141–51.
[47] Orif MI, Abdel-Rhman MH. Synthesis, spectral and structural studies on some new isonicotinic thiosemicarbazide complexes and its biological activity. Polyhedron 2015;98:162–79.
[48] El-Asmy AA, Rakha TH, Abdel-Rhman MH, Hassanien MM, Al-Mola AS. Synthesis, spectral, thermal and biological studies on N(2,4-dinitro-phenyl)-2-mercaptoacetohydrazide and its metal complexes. Spectrochim Acta A Mol Biomol Spectrosc 2015;136:1718–27.
[49] Nakamoto K. Infrared and Raman spectra of inorganic and coordination compounds. New York: Wiley Online Library; 1978.
[50] Lever ABP. Inorganic electronic spectroscopy. Amsterdam, Netherlands; 1968.
[51] Paleologos EK, Giokas DL, Karayannis MI. Micelle-mediated separation and cloud-point extraction. TrAC Trends Analyt Chem 2005;24(5):426–36.
[52] Laespada MEF, Pavón JLP, Cordero BM. Micelle-mediated methodology for the preconcentration of uranium prior to its determination by flow injection. Analyst 1993;118(2):209–12.
[53] Aranda PR, Gil RA, Moyano S, De Vito IE, Martinez LD. Cloud point extraction of mercury with PONPE 7.5 prior to its determination in biological samples by ETAAS. Talanta 2008;75(1):307–11.
[54] Liao P-H, Jiang S-J, Sahayam A. Cloud point extraction combined with flow injection vapor generation inductively coupled plasma mass spectrometry for preconcentration and determination of ultra trace Cd, Sb and Hg in water samples. J Anal At Spectrom 2012;27(9):1518–24.
[55] Garrido M, Di Nezio M, Lista A, Palomeque M, Fernández Band B. Cloud-point extraction/preconcentration on-line flow injection method for mercury determination. Anal Chim Acta 2004;502(2):173–7.
[56] Ulusoy Hİ, Gürkan R, Ulusoy S. Cloud point extraction and spectrophotometric determination of mercury species at trace levels in environmental samples. Talanta 2012;88:516–23.
[57] Bezerra MA, Mitihiro do Nascimento Maêda S, Oliveira EP, de Fátima Batista de Carvalho M, Santelli RE. Internal standardization for the determination of cadmium, cobalt, chromium and manganese in saline produced water from petroleum industry by inductively coupled plasma optical emission spectrometry after cloud point extraction. Spectrochim Acta Part B At Spectrosc 2007;62(9):985–91.
[58] Borkowska-Burnecka J, Szymczycha-Madeja A, Żyrnicki W. Determination of toxic and other trace elements in calcium-rich materials using cloud point extraction and inductively coupled plasma emission spectrometry. J Hazard Mater 2010;182(1):477–83.